JOURNAL OF SOLID STATE CHEMISTRY **123,** 408–412 (1996)
ARTICLE NO. 0196

BRIEF COMMUNICATION

Three-Dimensional Metal Piperazinyldiphosphonate Phases with Ellipsoidal Cavities Defined by 44-Membered Rings: Crystal Structures of $[M\{O_3PCH_2NH(C_2H_4)_2NHCH_2PO_3\}] \cdot H_2O$, M = Mn and Co

Robert LaDuca,* David Rose,* Jeffrey R. D. DeBord,*,† Robert C. Haushalter,† Charles J. O'Connor,‡ and Jon Zubieta,*

*Department of Chemistry, Syracuse University, Syracuse, New York 13244; †NEC Research Institute, 4 Independence Way, Princeton, New Jersey 08540; and ‡Department of Chemistry, University of New Orleans, New Orleans, Louisiana 70148

Received January 17, 1996; accepted February 15, 1996

The hydrothermal reaction of a mixture of $(Et_4N)_2MnCl_4$, *N*, *N′*-piperazinebis(methylenephosphonic acid), $Et_4NCl \cdot H_2O$, and H_2O in the mole ratio 1 : 1 : 5 : 300, adjusted to pH 5 with 40% aqueous $(Bu_4N)OH$, at 160°C for 63 h yielded $[Mn\{O_3PCH_2NH(C_2H_4)_2NHCH_2PO_3\}] \cdot H_2O$ (1) in 60% as off-white platelets. The analogous reaction using $(Et_4N)_2CoCl_4$ produced $[Co\{O_3PCH_2NH(C_2H_4)_2NHCH_2PO_3\}] \cdot H_2O$ (2). The isomorphous materials 1 and 2 display three-dimensional network structures, based on binuclear units of corner-sharing metal and phosphorus tetrahedra, forming eight membered $\{-Co-O-P-O-\}_2$ rings. The diphosphonate groups serve to tether the binuclear units into large ellipsoidal 44-membered rings. As the piperazinyl nitrogen atoms are protonated, the organic moiety of the disphosphonate group serves as both tether and charge compensating site. Compound 1 exhibits Curie–Weiss paramagnetism with weak antiferromagnetism between Mn centers. In contrast, the susceptibility of 2 exhibits a broad maximum at low temperatures consistent with short range antiferromagnetic coupling. Crystal data: 1, $C_6H_{16}MnN_2O_7P_2$, triclinic $P\bar{1}$, a = 8.393(2)Å, b = 9.043(2)Å, c = 9.125(2)Å, α = 62.88(3)°, β = 86.36(3)°, γ = 78.96(3)°, V = 604.8(3)Å^3; R = 0.056 for 1663 reflections. 2, $C_6H_{16}CoN_2O_7P_2$, triclinic $P\bar{1}$, a = 8.340(2)Å, b = 8.917(2)Å, c = 9.018(2)Å, α = 64.11(3)°, β = 86.24(3)°, γ = 78.87(3)°, V = 591.9(2)Å^3; R = 0.083 for 1917 reflections.

The recent acceleration in the development of metal organophosphonates stems not only from their expansive coordination chemistry (1–3) but also from their practical applications as catalysts, hosts in intercalation compounds, sorbents, ion-exchangers, protonic conductors, and components in the preparation of films possessing optical, nonlinear optical, or electronic properties (4–17). While metal organophosphonate phases possessing two-dimensional structures offer a recurring structural theme (18–21), three-dimensional zeolite-like phosphonate structures have been reported recently for β-$Cu(O_3PCH_3)$ (22) and $Zn(O_3PC_2H_4NH_2)$ (23).

One strategy for expanding the structural chemistry of metal phosphonate phases involves the used of diphosphonic acids $H_2O_3P-R-PO_3H_2$ or of functionalized phosphonic acids such as $H_2O_3PCH_2CH_2COOH$, as in the preparation of pillared layered structures of zirconium (24), vanadium (25–27), zinc (28), bismuth (29), and mixed manganese/zinc phases (30). We have noted that modifications in the tether length R of a diphosphonate may influence not only the layer separation distance in two-dimensional phases but may also dictate the dimensionality of the solid (25). Furthermore, the tether itself may be "sculpted" to allow variations in the dimensions of the interlamellar void space or may be functionalized to provide portonation sites or additional coordination sites. One such designed diphosphonic acid, *N*, *N′*-piperazinebis (methylenephosphonic acid), has been shown to act as both cation and diphosphonate tether in the pillared layer structure of $[(VO)(H_2O)\{O_3PCH_2NH(C_2H_4)_2NHPO_3\}]$ (26). In an effort to extend the chemistry of this unique diphosphonate group, the chemistry with Mn and Co was investigated, resulting in the isolation of open framework three-dimensional phases $[M\{O_3PCH_2NH(C_2H_4)_2NHCH_2PO_3\}] \cdot H_2O$ (M = Mn (**1**) and Co (**2**)) with large ellipsoidal cavities defined by 44-membered rings.

0022-4596/96 $18.00

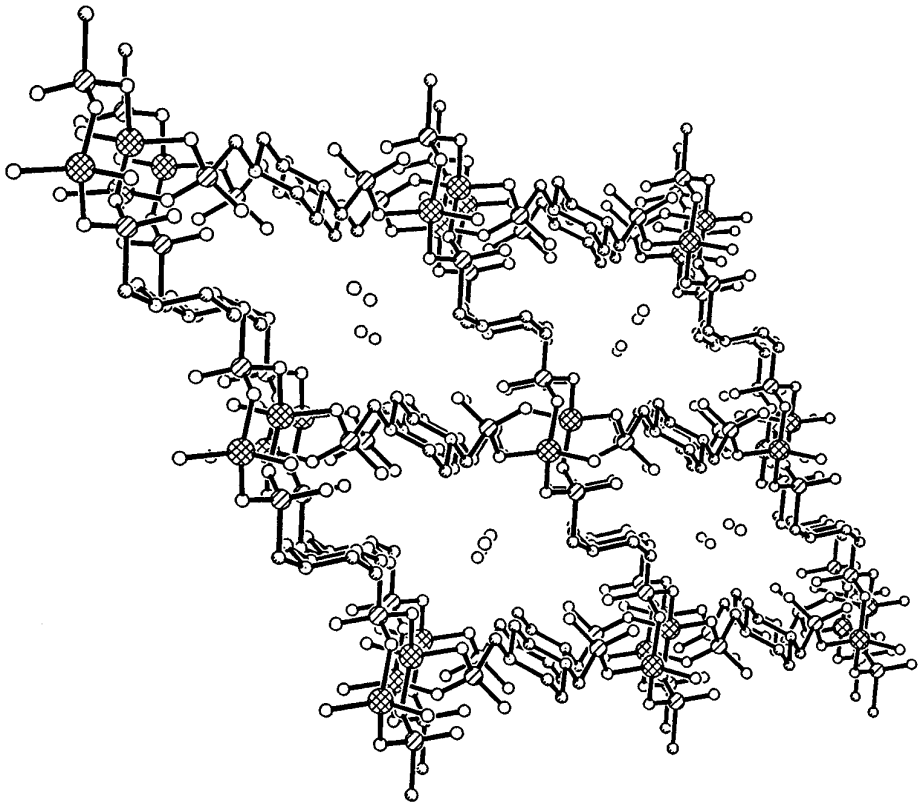

FIG. 1. A view of the structure of $[Co\{O_3PCH_2NH(C_2H_4)_2NHCH_2PO_3\}] \cdot H_2O$ (**2**), viewed down the crystallographic [100] direction, showing the cavities occupied by water molecules. Co sites are cross-hatched circles; P, striped left to right; O, open; C, lightly shaded.

The hydrothermal reaction of a mixture of $(Et_4N)_2CoCl_4$, *N*, *N*′-piperazinebis(methylenephosphonic acid), $Et_4NCl \cdot H_2O$, and H_2O at 160°C for 63 h afforded blue plates of $[Co\{O_3PCH_2NH(C_2H_4)_2NHCH_2PO_3\}] \cdot H_2O$ (**2**) in 80% yield (31). Compound **1**, $[Mn\{O_3PCH_2NH(C_2H_4)_2NHCH_2PO_3\}] \cdot H_2O$, was prepared in an analogous fashion from $(Et_4N)_2MnCl_4$.

Compound **2** is best described as a three-dimensional Co–O–P–C covalently lined network solid (32). The cobalt site exhibits tetrahedral geometry, with each vertex defined by an oxygen from each of four different diphosphonate ligands. Each $\{\text{-}RPO_3\}$-terminus of the diphosphonate ligands coordinates to two Co sites through two oxygen donors resulting in a pendant {P = O} moiety at each phosphorus site.

The extended structure of **2**, shown in Fig. 1, is based upon two cobalt tetrahedra corner-sharing with two phosphorus tetrahedra, to form an eight membered $\{\text{–Co–O–P–O–}\}_2$ ring, which adopts a pseudo-chair conformation. Within a dimer, the cobalt atoms are linked by the bidentate $\{RPO_3\}$-terminus of two crystallographically identical diphosphonate linkages. The metal dimer units are connected to neighboring metal sites through the organodiphosphonate groups resulting in undulating sheets constructed of cobalt/PO_3 dimers linked into chains which are in turn connected through $\{CH_2NH(C_2H_4)_2NHCH_2\}^{2+}$ tethers (Fig. 2). These sheets are then connected to those above and below the sheet plane through two identical $(O_3PCH_2NH(C_2H_4)_2NHCH_2PO_3)^{2-}$ units, resulting in 44-membered rings which form the boundaries for large elliptical voids (Fig. 3).

The structure-directing role of the piperazinyl moiety is manifested in the shape of the cavities which is dictated in part by the chair conformation of the piperazinyl structural units. The approximate dimensions of the ellipsoidal cavity are 4.7Å by 18.0Å. The water molecules of hydration are accommodated within these spacious cavities.

The water molecules of hydration are hydrogen-bonded to the phosphate oxygen atoms of the Co–P–O framework with O7 · · · O1 and O7 · · · O5 distances of 2.94(1)Å and 2.85(1)Å, respectively. Similarly, the piperazinyl protons engage in hydrogen bonding to the pendant {P = O} groups of the phosphate termini of the diphosphonate moieties.

Compound **1** is isomorphous with **2**, exhibiting only minor variations in metrical parameters. The most significant difference is the contraction of the average *M*–O bond

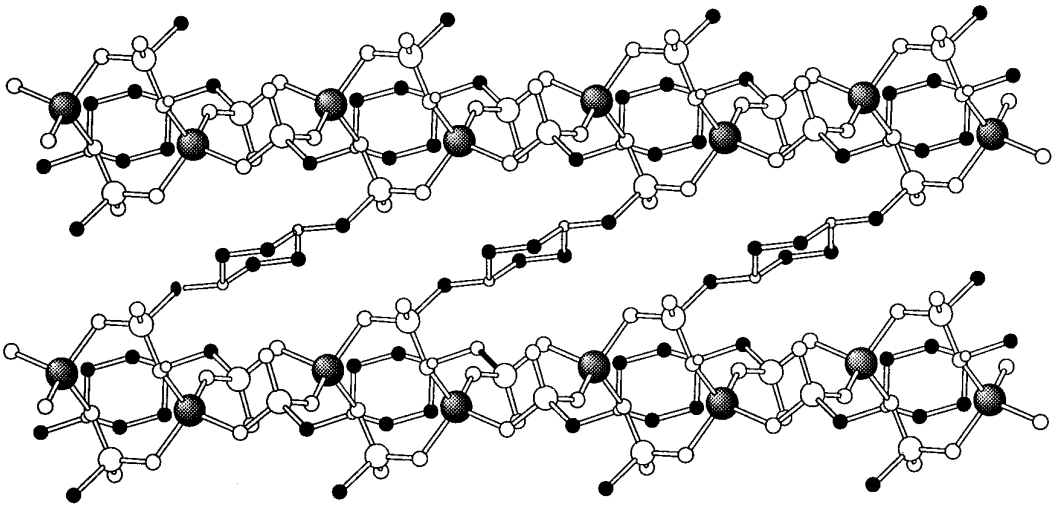

FIG. 2. A view of the structure of **2**, showing the chains of corner-sharing $\{CoO_4\}$ and $\{PO_3C\}$ tetrahedra, linked through the $\{NH(C_2H_4)_2NH\}^{2+}$ tethers of the diphosphonate groups. Co sites are heavily shaded, circles; P, large open circles; O, small open; N, smallest open; C, filled in.

distance from 2.031(8)Å in **1** to 1.950(9)Å in **2**, a feature consistent with the trend in covalent radii for the *d*-block elements.

The temperature dependent magnetic susceptibility data for both compounds exhibit Curie–Weiss paramagnetism at high temperatures (33). The magnetic data for the two compounds were fit to the Curie–Weiss law,

$$\chi = C/(T - \theta) = Ng^2\mu_B^2 S(S + 1)/[3k(T - \theta)]. \quad [1]$$

For the Mn(II) material (**1**), the inverse magnetic susceptibility plot provided least-squares fitted parameters C = 4.06 emu K mol^{-1} and $\theta = -5.71$ K. The negative θ is consistent with a weak antiferromagnetic coupling between the manganese centers. The electron structure of the complex corresponds to manganese(II) as the $3d^5$ electron structure, which gives a g-value for the $S = 5/2$ compound corresponding to $g = 1.93$.

The magnetic susceptibility data for **2** were fit to the Curie–Weiss law at higher temperatures ($T > 100$ K) with the fitted parameters $C = 2.70$ emu K/mol, $\theta = -8.268$ K, and TIP = 0.000321 emu/mole. The inverse magnetic susceptibility data are plotted in the inset of Fig. 4 with the fitted curve. As shown in the figure, at lower tempera-

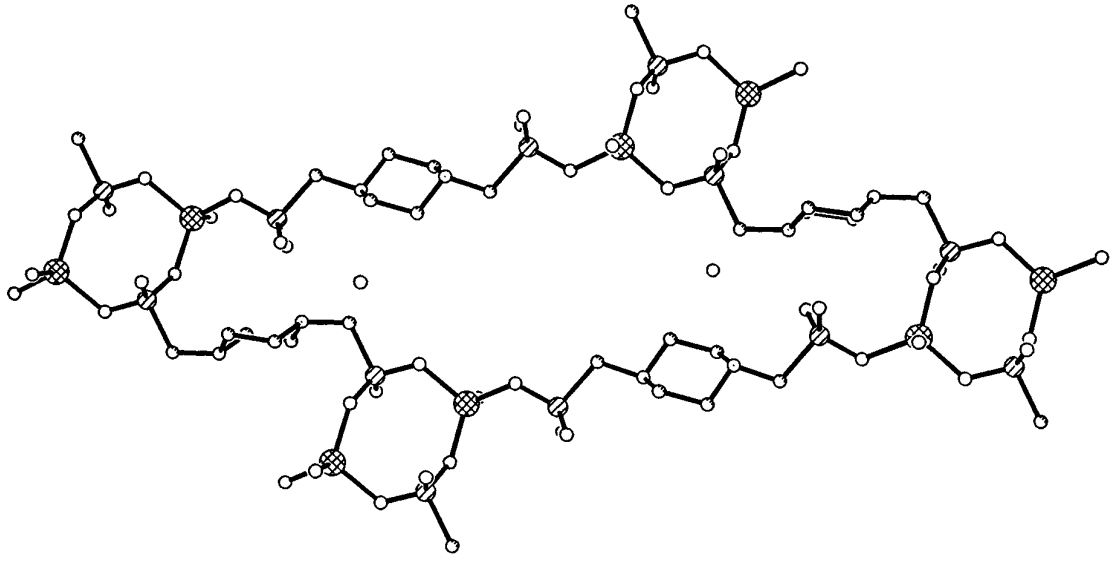

FIG. 3. A view down the [111] direction showing the large 44-membered ellipsoidal rings which provide a structural motif for **1** and **2**.

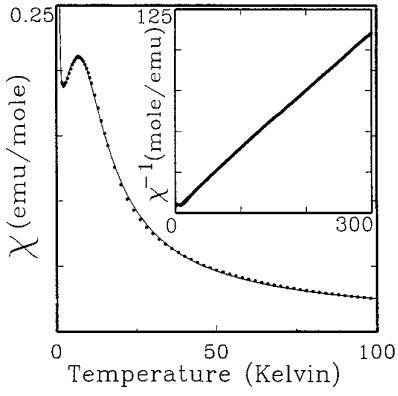

FIG. 4. The magnetic susceptibility of $[Co\{O_3PCH_2HN(C_2H_4)_2NHCH_2PO_3\}] \cdot H_2O$ (**2**) plotted as a function of temperature over the 1.7–100 K temperature region. The curve drawn through the data is the fit to the binuclear model as described in the text. The inset illustrates the inverse magnetic susceptibility plotted as a function of temperature over the 1.7–300 K temperature region. The line drawn through the data in the inset is the fit to the Curie–Weiss model as described in the text.

tures, the magnetic susceptibility exhibits a broad maximum consistent with short range antiferrogmagnetic coupling. The magnetic data were analyzed in the vicinity of the maximum using a model that assumes coupling of two $S = 3/2$ Co(II) centers (35). The magnetic data also required a correction using the molecular field approximation due to secondary interactions, either from interdimer coupling, or from zero field splitting of the $S = 3/2$ multiplet (36). The addition of the molecular field exchange correction resulted in a substantial improvement of the fit to the data, with the following parameters: $J/k = -2.6$ K, $zJ'/k = -2.7$, and TIP = 0.0063.

REFERENCES

1. J. Zubieta, *Comments Inorg. Chem.* **16,** 153 (1994), and references therein.
2. Q. Chen, J. Salta, J. Zubieta, *Inorg. Chem.* **32,** 4485 (1993).
3. C. Bhardwaj, H. Hu, and A. Clearfield, *Inorg. Chem.* **32,** 4294 (1993), and references therein.
4. G. Alberti, U. Constantino, F. Marmottini, R. Vivani, and P. Zappelli, *Angew. Chem.* **105,** 1396 (1993); *Angew. Chem. Int. Ed. Engl.* **32,** 1357 (1993), and references therein.
5. G. Alberti, U. Constantino, *in* "Inclusion Compounds" (J. L. Atwood, J. E. D. Davis, and D. D. MacNicol, Eds.), Vol. 5, Chap. 5. Oxford Univ. Press, London/New York, 1991.
6. D. A. Burwell and M. E. Thompson, *in* "Supramolecular Architecture," *ACS Sympos. Ser.* **499,** 166 (1992).
7. A. Clearfield and C. Y. Ortiz-Avila, *in* "Supramolecular Architecture," *ACS Sympos. Ser.* **499,** 178 (1992).
8. A. Clearfield, "Inorganic Ion Exchange Materials." CRC Press, Boca Raton, FL, 1982.
9. A. Clearfield, *in* "Design of New Materials" (D. L. Cocke and A. Clearfield, Eds.). Plenum, New York, 1986.
10. G. L. Rosenthal and J. Caruso, *Inorg. Chem.* **31,** 144 (1992).
11. Y. Zhang and A. Clearfield, *Inorg. Chem.* **31,** 2821 (1992).
12. D. A. Burwell, K. G. Valentine, J. H. Timmermans, and M. E. Thompson, *J. Am. Chem. Soc.* **114,** 4144 (1992).
13. G. Gao and T. E. Mallouk, *Inorg. Chem.* **30,** 1434 (1991).
14. R-C. Wang, Y. Zhang, H. Hu, R. R. Frausto, and A. Clearfield, *Chem. Mater.* **4,** 864 (1992).
15. H. E. Katz, W. L. Wilson, and G. Scheller, *J. Am. Chem. Soc.* **116,** 6636 (1994).
16. S. B. Ungashe, W. L. Wilson, H. E. Katz, G. R. Scheller, and T. M. Putrinski, *J. Am. Chem. Soc.* **114,** 8717 (1992).
17. H. Byrd, J. K. Pike, and D. R. Talham, *J. Am. Chem. Soc.* **116,** 7903 (1994).
18. J. W. Johnson, A. J. Jacobson, W. M. Butler, S. E. Rosenthal, J. F. Brody, and J. T. Lewandowski, *J. Am. Chem. Soc.* **111,** 381 (1989).
19. G. H. Huan, A. J. Jacobson, J. W. Johnson, and E. W. Corcoran, Jr., *Chem. Mater.* **2,** 2 (1990).
20. G. H. Huan, J. W. Johnson, A. J. Jacobson, and J. S. Merola, *J. Solid State Chem.* **89,** 220 (1990).
21. G. H. Huan, A. J. Jacobson, J. W. Johnson, and D. P. Goshorn, *Chem. Mater.* **4,** 661 (1992).
22. J. LeBideau, C. Payen, P. Palvadeau, and B. Bujoli, *Inorg. Chem.* **33,** 4885 (1994).
23. S. Drumel, P. Janvier, D. Deniaud, and B. Bujoli, *J. Chem. Soc. Chem. Commun.,* 1051 (1995).
24. M. B. Dines, R. E. Cooksey, P. C. Griffith, and R. H. Lane, *Inorg. Chem.* **22,** 1003 (1983); G. Alberti, U. Costantino, F. Marmottini, R. Vivani, and P. Zappelli, *Angew. Chem. Int. Ed. Engl.* **32,** 1357 (1993); G. Alberti, F. Marmottini, S. Murcia-Mascaros, and R. Vivani, *Angew. Chem. Int. Ed. Engl.* **33,** 1594 (1994); L. A. Vermeulen and M. E. Thompson, *Chem. Mater.* **6,** 77 (1994); E. W. Stein, C. Bhardwaj, C. Y. Ortiz-Avila, A. Clearfield, and M. A. Subramanian, *in* "Materials Science Forum," Vols. 152, 153. Trans. Tech. Publ., Switzerland, 1994; Katz, H. E., *Chem. Mater.* **6,** 2227 (1994); G. Cao, H. Hong, and T. E. Mallouk, *Acc. Chem. Reg.* **25,** 420 (1992).
25. V. Soghomonian, Q. Chen, R. C. Haushalter, and J. Zubieta, *Angew. Chem. Int. Ed. Engl.* **34,** 223 (1995).
26. V. Soghomonian, R. Diaz, R. C. Haushalter, C. J. O'Connor, and J. Zubieta, *Inorg. Chem.,* in press (1995).
27. V. Soghomonian, R. C. Haushalter, and J. Zubieta, *Chem. Mater.,* in press (1995).
28. S. Drumel, P. Janvier, P. Barboux, M. Bujoli-Doeuff, and B. Bujoli, *Inorg. Chem.* **34,** 148 (1995).
29. P. Janvier, S. Drumel, Y. Piffard, and B. Bujoli, *C.R. Acad. Sci. Paris, Ser. 2* **320,** 29 (1995).
30. S. Drumel, P. Janvier, M. Bujoli-Doeuff, and B. Bujoli, *New J. Chem.* **19,** 239 (1995).
31. A mixture of $(Et_4N)_2CoCl_4$ (0.51 mmol), *N*, *N*′-piperazinebis (methylenephosphonic acid), tetraethylammonium chloride hydrate, and deionized water in the mole ratio 1 : 1 : 5 : 300 was adjusted to pH 5 with 40% aqueous tetraethylammonium hydroxide and heated at 160°C for 63 hr in a Parr acid digestion bomb. Blue platelets of **1** were isolated as a monophasic material in greater than 80% yield. Compound **2** was prepared as off-white platelets under the same reaction conditions, using $(Et_4N)_2MnCl_4$ as the metal source. Attempts to prepare the analogous Fe compound from $(Et_4N)_2FeCl_4$ failed to produce crystalline products. IR(KBr pellet, cm^{-1}): **1**, 3398(s, br), 2950 (w), 1676(w), 1452(m), 1263(s), 1074(s), 995(s), 962(m), 778(w). **2**, 3467(s, br), 3023 (w), 2990(w), 1663(m), 1522(m), 1437(m), 1069(s), 993(s), 960(m), 780(m), 567(m), 545(m).
32. Crystal Data: $C_6H_{16}MnN_2O_7P_2$ (**1**), triclinic, $P\bar{1}$, $a = 8.393(2)$Å, $b = 9.043(2)$Å, $c = 9.125(2)$Å, $\alpha = 62.88(3)°$, $\beta = 86.36(3)°$, $\gamma = 78.96(3)°$, $V = 604,8(3)$Å^3, $Z = 2$, $D_c = 1.895$g cm^{-3}, $Z = 2$, $\mu = 1.381$ mm^{-1}, $T = 233$ K; structure solution and refinement based on 1663 reflections with $I_0 \geq 3\sigma(I_0)$ converged at $R = 0.056$. $C_6H_{16}CoN_2O_7P_2$ (**2**), triclinic, $P1$, $a = 8.340(2)$Å, $b = 8.917(2)$Å, $c = 9.018(2)$Å, $\alpha = 64.11(3)°$,

β = 86.24(3)°, γ = 78.87(3)°, V = 591.9(3)Å^3, D_c = 1.959g cm^{-3}, Z = 2, μ = 1.749 mm^{-1}, T = 233 K; structure solution and refinement based on 1917 reflections with $I_0 \geq 3\sigma(I_0)$ converged at R = 0.083. In both cases, data was collected on a Rigaku AFC-5S diffractometer using graphite crystal-monochromated Mo$K\alpha$ radiation (λ = 0.71073Å) with 2θ–ω scans. An empirical absorption correction was applied. The structure was determined by direct methods using the SHLEXTL PLUS solution and refinement programs. All non-hydrogen atoms were defined anisotropically; hydrogen atoms were located in idealized positions.

33. The magnetic susceptibility data were recorded from 33.27 mg and 46.35 mg polycrystalline samples of $Mn\{O_3PCH_2HN(CH_2)_4NHCH_2PO_3\} \cdot H_2O$ and $Co\{O_3PCH_2HN(CH_2)_4NHCH_2PO_3\} \cdot H_2O$, respectively, over the 2–300 K temperature range using a Quantum Design MPMS-5S SQUID susceptometer. Measurement and calibration techniques have been reported elsewhere (34). The temperature dependent magnetic data were measured at a magnetic field of 1000 G.
34. C. J. O'Connor, *Prog. Inorg. Chem.* **29,** 203 (1982).
35. The isotropic coupling of these two centers gives the following magnetic susceptibility equation

$$\chi = \frac{Ng^2\mu_B^2}{kT} \frac{e^{2J/kT} + 5e^{6J/kT} + 14e^{12J/kT}}{1 - 3e^{2J/kT} + 15e^{6J/kT} + 7e^{12J/kT}}.$$

36. The secondary interactions were treated using the molecular field approximation,

$$\chi = \frac{\chi'}{1 - (2zJ'/Ng^2\mu_B^2)\chi'},$$

where χ' is the magnetic susceptibility of the material in the absence of the exchange field and χ is the molecular exchange field influenced magnetic susceptibility that is actually measured. The exchange field coupling parameter is zJ', where z is the number of exchange coupled neighbors.